

Structure of the Room-Temperature Ionic Liquid/SiO₂ Interface Studied by Sum-Frequency Vibrational Spectroscopy

Brian D. Fitchett and John C. Conboy*

University of Utah, 315 South 1400 East, Salt Lake City, Utah 84112

Received: June 30, 2004; In Final Form: September 24, 2004

In the study presented here, the structure of the RTIL/SiO₂ interface has been examined by sum-frequency vibrational spectroscopy (SFVS). A series of hydrophobic RTILs composed of 1-alkyl-3-methylimidazolium (C_nmim, *n* = 6, 8 and 10) and bis(perfluoromethylsulfonyl)imide (BMSI) and bis(perfluoroethylsulfonyl)imide (BETI) anions have been examined. SFVS was used to determine the orientation of the cation as well as the structure of water at the RTIL/SiO₂ interface. The alkyl chain of the imidazolium cation was determined to be nearly normal to the surface for all the RTILs examined. The conformational order of the alkyl chain on the cation was also determined and was found to be dependent on the length of the alkyl chain, with longer chains being more ordered with few gauche defects. The tilt of the imidazolium ring with respect to the surface normal was also determined and was found to be ~28° for the BMSI salts with a reduction in the tilt angle to ~18° for the BETI RTILs. The water at the surface associated with the RTIL was determined to be hydrogen-bonded either singly or doubly to the anions at the SiO₂ interface. In addition, the nature of the hydrogen-bonding was found to be dependent on the amount of bulk water contained in the RTIL.

Introduction

Air- and water-stable room-temperature ionic liquids (RTILs) are a new class of materials with unique physical and chemical properties. RTILs have proven useful as solvents for electrochemistry,^{1–7} organic synthesis,^{8–12} catalysis,^{12–18} and extractions.^{18–28} Many RTILs are composed of bulky asymmetric organic cations, such as *N*-alkylpyridinium, tetraalkylammonium, and *N,N'*-dialkylimidazolium. Some of the most common air- and water-stable RTILs are composed of *N,N'*-dialkylimidazolium in combination with a variety of anions, including halides, tetrafluoroborate (BF₄[−]), hexafluorophosphate (PF₆[−]), hexafluoroarsenate (AsF₆[−]), nitrate, triflate (CF₃SO₃[−]), tris(perfluoroalkylsulfonyl) methides [(C_nF_{2n+1}SO₂)₃C[−]], and bis(perfluoroalkylsulfonyl)imides. Many of these RTILs have been characterized extensively with regard to their bulk physical and chemical properties.^{5,7,8,23,29–37}

In contrast to the growing information on the bulk properties of RTILs, very little is known of the interfacial structure of RTILs in contact with a solid, liquid, or gas. Previous reports of the RTIL interface have concentrated on the vacuum or gaseous interface as studied by direct recoil spectrometry,^{38–40} by X-ray^{41–43} and neutron diffraction.⁴¹ More recently, sum-frequency generation has been used to study both the RTIL/air and RTIL/platinum electrode interfaces.⁴⁴ The interfacial properties of the RTIL/solid interface are of general importance in areas such as heterogeneous reactions, heterogeneous catalysis, electrochemistry, and fuel cells. However, to make the most of RTILs for these particular applications, a more detailed understanding of the molecular structure of the interface is needed.

Our previous studies³⁷ focused on the bulk physical properties of a series of 1-*n*-alkyl-3-methylimidazolium (C_nmim, where *n* = 6, 8, and 10) bis(trifluoromethylsulfonyl)imide (BMSI) and bis(perfluoroethylsulfonyl)imide (BETI) RTILs, which are shown in Figure 1. We report here the first use of sum-frequency

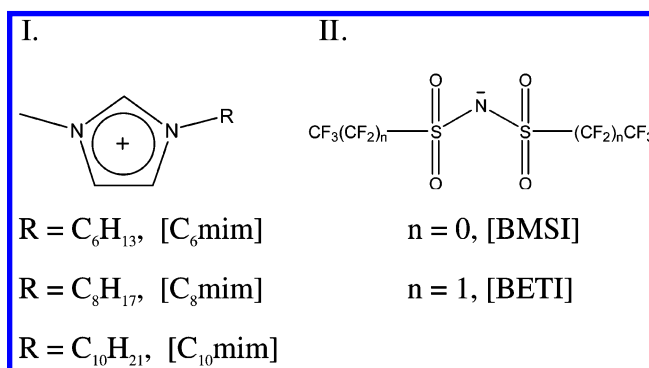


Figure 1. Structures of the imidazolium cations (I) and bis(perfluoroalkylsulfonyl)imide anions (II).

generation vibrational spectroscopy (SFVS) to investigate the interfacial molecular structure of these RTILs in contact with a fused silica surface. This unique class of RTILs represents some of the most hydrophobic water-immiscible RTILs reported. Although water-immiscible, these RTILs do contain a considerable amount of water both under ambient conditions (0.27–1.79 mol %) and upon equilibration with bulk water (14.0–23.3 mol %).³⁷ Surprisingly, RTIL water mixtures exhibit a substantially reduced water activity compared to salt solutions of similar concentrations.^{37,45,46} Although the bulk properties of these materials have been explored in detail, including the hydrogen bonding of water in this unique class of RTILs, little is known of their interfacial properties. The reduced water activity and the amphiphilic nature of the imidazolium cation suggest that the interfacial molecular structure and composition of these materials might be considerably different from that found at a typical liquid/solid interface.

Sum-Frequency Vibrational Spectroscopy. SFVS has been used here to study the structure of the RTIL/SiO₂ interface. SFVS is a second-order nonlinear optical spectroscopy, which has the chemical selectivity of IR and Raman spectroscopy and is inherently surface specific in nature. The details of SFVS

* Corresponding author. E-mail: conboy@chem.utah.edu.

have been described in detail elsewhere.⁴⁷ Experimentally, SFVS is performed by overlapping, both spatially and temporally, a visible and tunable IR source on a surface where they combine to produce a third photon at the sum of their respective frequencies. SFVS only occurs in systems that do not possess inversion symmetry. Since an interface or surface breaks the inversion symmetry of an isotropic media, SFVS is observed. The intensity of the SFVS signal, I_{SF} , is given by

$$I_{\text{SF}} = |\tilde{f}_{\text{SF}} f_{\text{vis}} f_{\text{IR}} \chi^{(2)}|^2 \quad (1)$$

where $\chi^{(2)}$ is the second-order nonlinear susceptibility tensor and \tilde{f}_{SF} , f_{vis} , and f_{IR} are the geometric Fresnel coefficients for the sum, visible, and IR fields, respectively. The nonlinear susceptibility tensor, $\chi^{(2)}$, is the sum of a resonant (R) contribution and a nonresonant (NR) contribution given by

$$\chi^{(2)} = \chi_{\text{NR}}^{(2)} + \sum_{\nu} \chi_{\text{R}}^{(2)} \quad (2)$$

with the resonant contribution defined as

$$\chi_{\text{R}}^{(2)} = \frac{N \langle A_k M_{ij} \rangle}{\omega_{\nu} - \omega_{\text{IR}} - i\Gamma_{\nu}} \quad (3)$$

where N is the number density at the surface, A_k is the IR transition probability, M_{ij} is the Raman transition probability, ω_{ν} is the frequency of the input IR field, ω_{IR} is the normal mode frequency of the vibrational transition, and Γ_{ν} is the line width of the transition. The brackets in eq 3 represent an average over all orientations. Examination of eq 3 shows that in order for a transition to be SFVS active, it must be both IR and Raman active.

One of the advantages of using SFVS is its ability to determine the orientation of molecules at the surface. To probe the component of a transition that is parallel to the surface normal, the ssp polarization combination (s-polarized sum-frequency, s-polarized visible, and p-polarized IR) is used, while transitions perpendicular to the surface normal are measured with the sps polarization combination (s-polarized sum-frequency, p-polarized visible, and s-polarized IR). Analysis of the transition strengths for both of these polarization combinations allows one to determine the orientation of a particular functional group in a molecule residing at the surface. By determining the orientation of several chemically distinct portions of a molecule, with independent vibrational frequencies, a complete picture of the structure of a complex molecule, such as the imidazolium cation of a RTIL, can be determined.

Experimental Section

The RTILs used in this study were synthesized via the procedure outlined previously.³⁷ Briefly, *n*-bromoalkanes (C_6 , C_8 , and C_{10}) (Sigma) were reacted with distilled 1-methylimidazole (Sigma) in the presence of K_2CO_3 . The resulting 1-alkyl-3-methylimidazolium bromides were dissolved in Nanopure (Barnstead) water and mixed with an aqueous solution of the anion (BMSI or BETI). The resulting colorless and transparent RTILs were washed with Nanopure water to remove any unreacted salts. The RTILs prepared by this method were C_6 -mim BMSI, C_8 mim BMSI, C_{10} mim BMSI, C_6 mim BETI, C_8 -mim BETI, and C_{10} mim BETI. In addition, C_8 mim-*d*₂₀ BMSI was also synthesized using $\text{C}_8\text{D}_{17}\text{Br}$ (98% D, Isotec). The resulting RTIL was reacted with NaOD (48% w/w in D_2O , Cambridge Isotope Laboratories, Inc.) to deuterate the imidazolium ring at positions 2, 4, and 5.⁴⁸ Excess NaOD was

neutralized with D_3PO_4 , and the RTIL was washed several times with D_2O to remove the excess salts. The resulting RTILs were dried under reduced pressure and either equilibrated with D_2O (99.9% D, Cambridge Isotope Laboratories, Inc.) or Nanopure water or used under ambient conditions.³⁷

Infrared spectra of the neat RTILs were obtained on a Spectrum One Fourier transform infrared (FTIR) spectrophotometer (Perkin-Elmer) equipped with a ZnSe attenuated total reflection (ATR) accessory (Pike Technologies) with a sample volume of 100 μL . Polarized Raman spectra of the neat RTILs were taken using the 647 nm line of a Kr-ion laser (Coherent). The RTILs were placed in a 1 cm fused silica cuvette and excited through the bottom of the cell. The scattered Raman light was detected perpendicular to the sample cell using a Spex F4 spectrograph and a charge-coupled device (CCD, Andor). Raman depolarization ratios were determined by placing a CaF_2 GlanTaylor polarizer (CASIX) before the detector to select the scattered light either parallel (0°) or perpendicular (90°) to the incident polarization. A depolarizer was placed after the polarizer to remove any bias in the detection system. The Raman depolarization ratio, ρ , was calculated from

$$\rho = \frac{I_{90^\circ}}{I_0} \quad (4)$$

where I_{90° and I_0 are the Raman intensity perpendicular and parallel to the excitation polarization, respectively.

The laser system used in the SFVS experiments was a tunable IR OPO/OPA (Laser Vision) pumped with the 1064 nm output of a pulsed nanosecond Nd:YAG laser (Surelite II, Continuum) with a 7 ns pulse width at a pulse rate of 10 Hz and a power of 500 mJ/pulse. The tuning range of the OPO/OPA used was 2800–4000 cm^{-1} . The output energy of the IR system used was 4 mJ/pulse at 3000 cm^{-1} with a beam size of 4 mm^2 . The visible beam was produced by frequency doubling of the 1064 nm Nd:YAG fundamental to produce 532 nm visible light. The output energy of the visible light was 3 mJ/pulse with a spot size of 4 mm^2 . The IR and visible beams were incident on the surface at an angle of 74 and 80°, respectively. All the SFVS experiments presented here were performed in a total internal reflection (TIR) geometry.⁴⁹ The resulting SFVS signal was filtered to remove the residual 532 nm light and measured with a photomultiplier tube (Hamamatsu) and gated electronics.

The cell used for the SFVS experiments consisted of a hemicylindrical IR grade fused silica prism (Almaz Optics) mounted on a custom-made Teflon cell with a fixed volume of ~1 mL. The silica prism and the cell were rinsed with acetone, blown dry with N_2 , and then cleaned in piranha solution (3:1 concentrated $\text{H}_2\text{SO}_4/30\% \text{H}_2\text{O}_2$) overnight. *Care must be taken when using piranha solution, as it is a strong oxidant and highly corrosive; avoid contact with organic solvents to prevent the formation of explosive products.* Both the prism and the Teflon cell were rinsed with copious amounts of Nanopure water. The prism was then further cleaned using a plasma cleaner (Harrick Scientific) with an Ar^+ plasma for 2 min. The plasma treatment does not appear to significantly etch the silica prism, as evidenced by the reproducibility of the measured spectra over the course of the experiments.

Results and Discussion

SFVS Vibrational Mode Assignments. Representative SFVS spectra of the water-equilibrated RTILs (equilibrated in D_2O) at the SiO_2 interface collected with ssp and sps polarization are shown in Figures 2 and 3, respectively. On the basis of previous

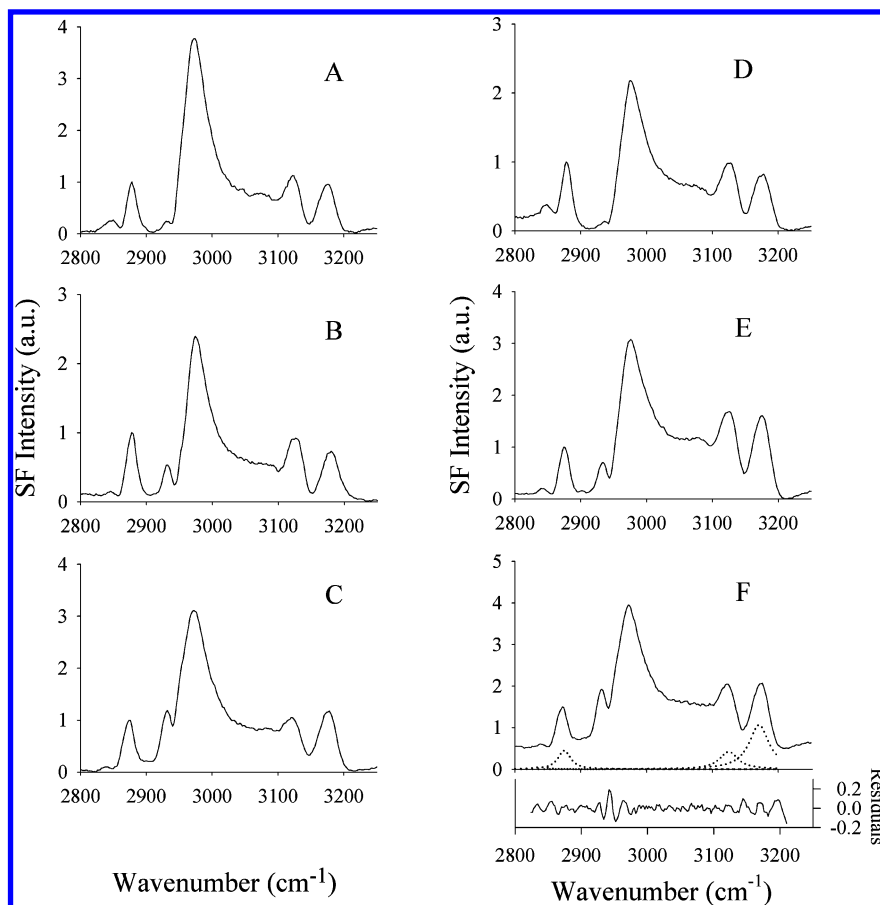


Figure 2. SFVS spectra of C₆mim BMSI (A), C₈mim BMSI (B), C₁₀mim BMSI (C), C₆mim BETI (D), C₈mim BETI (E), and C₁₀mim BETI (F, offset by 0.5) recorded with ssp polarization combination. C₁₀mim BETI (F) shows the spectral fits for the peaks (dotted lines) used in the conformational analysis of the imidazolium cation (other peaks omitted for clarity) as well as the residuals based on fits to eq 3. All spectra are normalized to the CH₃ ν_s peak at 2875 cm⁻¹.

measurements of water content,³⁷ the RTILs contain a considerable amount of D₂O, ranging from 23.3 mol % for C₆mim BMSI to 14 mol % for C₁₀mim BETI. The SFVS spectra displayed are an average of three samples and have been normalized to the CH₃ symmetric stretch (ν_s) at 2875 cm⁻¹ from the ssp spectra. The resonances observed in the spectra arise from the imidazolium cation; no resonances are observed from the perfluorinated anions in this spectral region. Three characteristic normal modes of the *n*-alkyl chain of the imidazolium cation are clearly visible: the CH₂ symmetric stretch (ν_s) at 2842 cm⁻¹ and the CH₃ ν_s and CH₃ Fermi resonance (ν_{FR}) at 2875 and 2930 cm⁻¹, respectively.^{50,51} The band at 2970 cm⁻¹ is a combination of the CH₃ antisymmetric stretch (ν_{as}) at 2950 cm⁻¹ and the N-CH₃ ν_s at 2991 cm⁻¹.^{52,53} The imidazolium ring produces two characteristic resonances at 3125 and 3175 cm⁻¹ associated with the HCCH ν_{as} and ν_s modes, respectively, from the hydrogens at ring positions 4 and 5.^{54,55} The broad spectral feature between 3000 and 3100 cm⁻¹ is due to the C-H stretch from the hydrogen at ring position 2.^{52,54} Spectral assignments of the normal modes for the N-CH₃ group on the imidazolium ring were determined by measuring the SFVS spectrum of C₈-mim-*d*₂₀ BMSI, as shown in Figure 4. This spectrum was normalized to the CH₃ ν_s of the corresponding nondeuterated RTIL (C₈mim BMSI). As shown in Figure 4, there is a resonance at 2991 cm⁻¹ which arises from the N-CH₃ ν_s . Also seen is a small peak at ~2850 cm⁻¹ arising from the CH₂ ν_s from incomplete deuteration of the alkyl chain (98%).

The SFVS vibrational frequency assignments were verified using a combination of IR, Raman, and molecular dynamics

simulations using hybrid density functional theory, B3LYP/6-311+G(2d, 2p) in Gaussian 03 after geometry optimization,⁵⁶ the results of which are summarized in Table 1. For comparison, representative Raman and ATR-FTIR spectra of C₁₀mim BMSI are shown in Figure 5. The Raman and IR vibrational frequencies of the imidazolium cation correlate extremely well with those observed in the SFVS spectra. Assignment of the two ring modes at 3125 and 3175 cm⁻¹ was verified using the Raman depolarization ratios, ρ , of these resonances.⁵⁴ The peak at 3175 cm⁻¹ has a depolarization ratio of $\rho = 0.091 \pm 0.02$ corresponding to the fully polarized symmetric A_1 vibration of the C_{2v} point group, while the peak at 3125 cm⁻¹ has $\rho = 0.74 \pm 0.13$ which is consistent with a fully nonpolarized asymmetric B_1 vibration. On the basis of these measurements, the peaks at 3125 and 3175 cm⁻¹ have been assigned as the asymmetric and symmetric HCCH stretches, respectively. The simulations produce frequencies that are quite different from the measured spectra; however, they are in good agreement as to the relative positions of the various vibrational modes of the cation. The spectral assignments made here are also consistent with previous Raman and IR measurements of similar materials.^{54,55}

Orientation of the Imidazolium Cation at the RTIL/SiO₂ Interface. Zhang et al.⁵⁷ have shown previously that the orientation of a particular transition dipole moment can be calculated from two independent measurements of $\chi^{(2)}$ by using the SFVS polarization combinations ssp and sps. The tilt angle

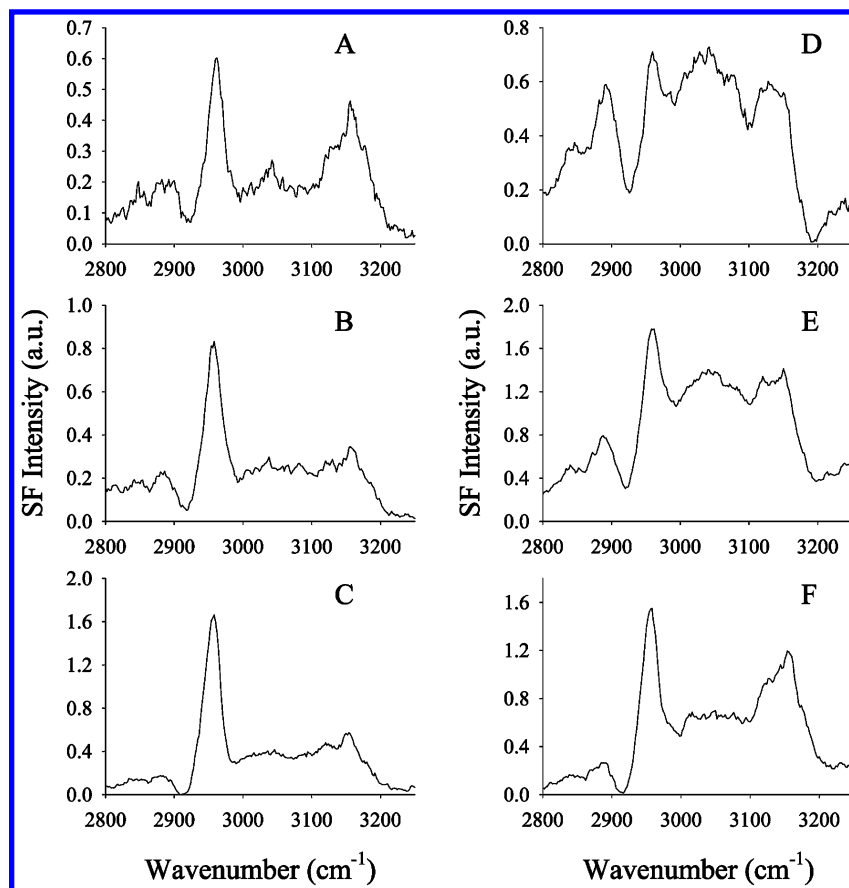


Figure 3. SFVS spectra of C₆mim BMSI (A), C₈mim BMSI (B), C₁₀mim BMSI (C), C₆mim BETI (D), C₈mim BETI (E), and C₁₀mim BETI (F) recorded with sps polarization combination. All spectra are normalized to the CH₃ ν_s peak at 2875 cm⁻¹ from the ssp spectra shown in Figure 2.

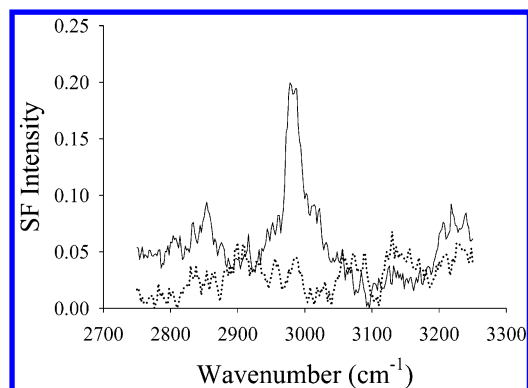


Figure 4. SFVS spectrum of C₈mim-d₂₀ BMSI recorded with ssp (solid line) and sps (dotted line) polarization combinations. The spectra are normalized to the CH₃ ν_s peak at 2875 cm⁻¹ of C₈mim BMSI.

of a particular transition moment with respect to the surface normal is given by

$$\theta = \arccot \left[\frac{\chi_{ssp}^{(2)} - \frac{1+R}{1-R} \frac{1-R}{2R}}{\chi_{sps}^{(2)}} \right]^{1/2} \quad (5)$$

where R is denoted by the following expressions

$$R = \frac{Q-1}{Q+2} \quad \text{or} \quad \frac{Q+1}{Q-2} \quad \text{and} \quad Q = \left[\frac{3}{5} \left(\frac{1}{\rho} - \frac{4}{3} \right) \right]^{1/2} \quad (6)$$

where ρ is the Raman depolarization ratio from eq 4. The appropriate value of R to be used in eq 5 is determined by an independent set of polarization measurements.⁵⁷ Both ssp (Figure 2) and sps (Figure 3) spectra of the RTILs were obtained in

TABLE 1: SFVS Vibrational Mode Assignments and Corresponding Values Obtained from IR and Raman Spectra and Calculated Using B3LYP/6-311+G(2d, 2p) in Gaussian 03 after Geometry Optimization⁵⁶ (Uncorrected Vibrational Frequencies Shown)^a

| peak assignments (cm ⁻¹) | SFVS | IR | Raman (ρ) | calcd |
|--------------------------------------|------|-------------------------|---|-------|
| CH ₂ ν _s | 2842 | 2857 | 2844 | 3023 |
| CH ₃ ν _s | 2875 | 2873 | 2862 (0.023) ⁵⁸ | 3036 |
| CH ₃ ν _{FR} | 2930 | 2928 | 2926 | |
| CH ₃ ν _{as} | 2950 | 2962 | 2954 | 3104 |
| N-CH ₃ ν _s | 2991 | | 2985 ⁵² (0.03) ⁵⁴ | 3077 |
| N-CH ₃ ν _{as} | | | 3025 ⁵² | |
| C(2)H ν _s | | | 3032 ⁵⁴ | |
| HC(4)C(5)H ν _{as} | 3125 | 3122 | 3114 (0.74) | 3279 |
| HC(4)C(5)H ν _s | 3175 | 3160 | 3167 (0.091) | 3296 |
| O-H ··· N (H-bonded) | 3510 | 3490 ⁶⁷ | | |
| H-O-H ν _s | | 3450-3657 ⁶⁸ | | |
| H-O-H ν _{as} | | 3520-3756 ⁶⁸ | | |
| free O-H | 3670 | | | |

^a The values in parentheses are the Raman depolarization ratios.

order to determine the orientation of the imidazolium cation at the SiO₂ interface.

Orientation of the *n*-Alkyl Chain. The SFVS spectra of the RTILs at the SiO₂ interface provide useful information regarding the orientation of the cations at the interface. Using the CH₃ ν_s intensity from the ssp and sps SFVS spectra and the Raman depolarization ratio of 0.023,⁵⁸ the tilt angle of the alkyl -CH₃ group, with respect to the surface normal, can be calculated from eq 5. On the basis of these calculations, the -CH₃ group on the alkyl chain has a tilt angle ranging from 25 to 42° for the BETI salts with a nearly constant -CH₃ tilt angle of 37° measured for the BMSI salts (Table 2). On the basis of the measured tilt angles in Table 2, and assuming an all-trans

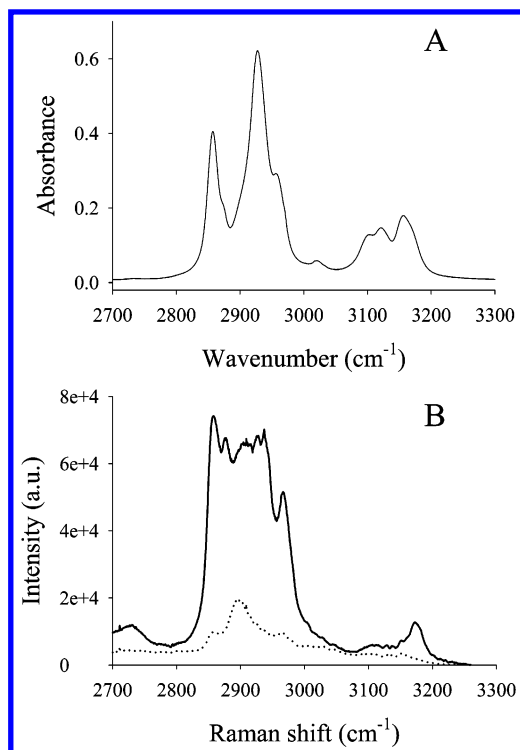


Figure 5. ATR-IR (A) and Raman (B) spectra of C₁₀mim BMSI. The solid line in part B is for the emission recorded at 0°, and the dotted line is for the emission recorded at 90° with respect to the incident polarization.

TABLE 2: Tilt Angles (in degrees) for the Terminal Methyl and Imidazolium Ring Determined from the SFVS Intensity Data

| | C ₆ mim BMSI | C ₈ mim BMSI | C ₁₀ mim BMSI | C ₆ mim BETI | C ₈ mim BETI | C ₁₀ mim BETI | C ₆ mim BMSI ^a | C ₁₀ mim BETI ^a |
|-------------------------------|-------------------------|-------------------------|--------------------------|-------------------------|-------------------------|--------------------------|--------------------------------------|---------------------------------------|
| -CH ₃ tilt | 36 ± 4 | 38 ± 8 | 39 ± 6 | 25 ± 5 | 32 ± 4 | 42 ± 10 | 32 ± 5 | 38 ± 6 |
| alkyl chain tilt ^b | 1 ± 4 | 3 ± 8 | 4 ± 6 | 10 ± 5 | 3 ± 4 | 7 ± 10 | 3 ± 5 | 3 ± 6 |
| HCCH tilt | 30 ± 4 | 21 ± 8 | 32 ± 5 | 16 ± 6 | 17 ± 5 | 20 ± 4 | 26 ± 5 | 23 ± 7 |

^a Values for the ambient RTILs, see text. ^b Assumes an all-trans chain conformation.

conformation, the alkyl chain on the imidazolium cation of the RTILs is pointing nearly perpendicular to the SiO₂ surface.

Conformation of the *n*-Alkyl Chain. While it is common in SFVS analyses to determine the orientation of an alkyl chain on the basis of the terminal methyl group,^{57,59,60} the conformation of the alkyl chain must also be considered. For the imidazolium cation, the peak intensities of the CH₂ ν_s and CH₃ ν_s at 2842 and 2875 cm⁻¹, respectively, can be used to obtain a relative measure of the conformational disorder of the *n*-alkyl chain.^{61–63} Examination of the spectra in Figure 2 reveals a reduction in the CH₂ ν_s/CH₃ ν_s intensity at ~2842 cm⁻¹ as the length of the alkyl chain on the cation is increased, for both the BMSI and BETI RTILs. The CH₂ ν_s/CH₃ ν_s peak intensity ratio for all the RTILs is summarized in Figure 6. The CH₂/CH₃ ratio decreases from 0.25 ± 0.01 for C₆mim BMSI and C₆mim BETI to 0.069 ± 0.013 for C₁₀mim BMSI and C₁₀mim BETI. These values suggest that the alkyl chains of the imidazolium cations of all the RTILs generally have few gauche defects and have a high degree of conformational order at the SiO₂ surface. It can be seen from Figure 6 that the length of the alkyl chain has a significant influence on the conformation of the alkyl chain. As the alkyl chain length is increased from C₆ to C₁₀, there is a marked reduction in the CH₂ ν_s/CH₃ ν_s intensity ratio which is indicative of a reduction in the number of gauche defects.

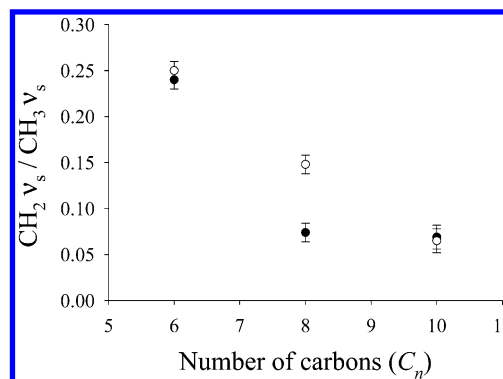


Figure 6. CH₂ ν_s/CH₃ ν_s ratio as a function of chain length for the BMSI RTILs (●) and the BETI RTILs (○).

For comparison, the RTILs are significantly more ordered than ionic surfactants at a variety of surfaces, which have a CH₂/CH₃ intensity ratio ranging from 0.6 to 7.^{61,63} Although it is not possible to quantify the number of gauche defects in the alkyl chains, the relatively small CH₂/CH₃ ratio measured for the RTILs suggests a high degree of conformational order, which supports the assumption made in the previous calculations that the alkyl chain is predominantly in an all-trans conformation.

Orientation of the Imidazolium Ring. One important feature of the spectra shown in Figures 2 and 3 is the presence of the HCCH antisymmetric and symmetric stretches from the imidazolium ring (Table 1). These two bands are also clearly seen in both the IR and Raman spectra (Figure 5). In a previous SFVS study of similar ionic liquids at the RTIL/air interface,⁴⁴ these ring modes were only present as very weak bands, which led to the conclusion that the imidazolium ring was lying parallel to the surface plane. In contrast, the ring modes displayed in Figure 2 are very prominent, suggesting that the imidazolium ring orientation is unlike that observed at the RTIL/air interface.

Since the HCCH stretches from the imidazolium ring are very intense in both the ssp and sps spectra, they can readily be used to calculate the tilt of the HCCH dipole. Using the HCCH ν_s at 3175 cm⁻¹ and the appropriate depolarization ratio from the polarized Raman experiments of 0.091 ± 0.02 (Table 1), the tilt angle of the HCCH ν_s dipole was calculated from eq 5. The resulting angles show that the HCCH ν_s dipole is tilted between 16° for C₆mim BETI and 32° for C₁₀mim BMSI from the surface normal. Previous studies involving the RTIL/air interface relied on both the symmetric and asymmetric HCCH stretches of the imidazolium ring to determine its orientation.⁴⁴ The HCCH ν_{as}, however, is completely depolarized (ρ = 0.74 ± 0.13) which gives no real solution for the tilt angle on the basis of eq 5.

Orientation of the N-CH₃ Group. The SFVS spectra of C₈mim-*d*₂₀ BMSI in both the ssp and sps polarization combinations are shown in Figure 4. By inspection of these spectra, the orientation of the N-CH₃ ν_s dipole lies predominantly parallel to the surface normal due to the lack of SFVS intensity seen in the sps polarization combination. However, the intensity of the ssp N-CH₃ ν_s (normalized to the intensity of the -CH₃ ν_s from C₈mim BMSI) is rather small, suggesting that there is a broad distribution of possible orientations.^{64,65} Ideally, the use of both the HCCH dipole and the N-CH₃ dipole orientations would allow for the determination of the tilt and twist of the imidazolium ring at the surface. However, there is no physical solution for the complete orientation of the ring (both tilt and twist) given the dipole orientations measured by SFVS, presumably due to the broad distribution of the N-CH₃ dipole. Due to the broad distribution of possible orientations for the N-CH₃

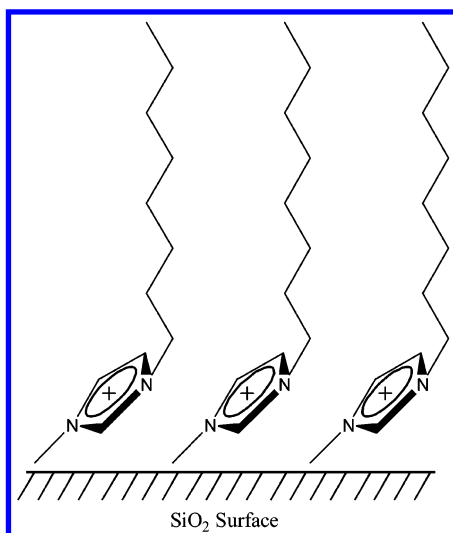


Figure 7. Schematic of the imidazolium cation orientation at the silica surface.

resonance, only the HCCH modes from the ring were used to determine the tilt of the imidazolium ring.

Complete Structure of the Imidazolium Cation at the RTIL/SiO₂ Interface. Figure 7 shows a schematic of the imidazolium cation structure at the SiO₂ surface obtained by combining the calculated and measured tilt angles from above and summarized in Table 2. An important conclusion drawn from the data presented in Table 2 is that there is very little change in the relative structure of the imidazolium cation upon alteration of the alkyl chain length or the anion (BETI versus BMSI). In addition to the RTIL composition, the influence of water content on the cation structure was also determined. The orientation of the imidazolium cations in ambient C₆mim BMSI and C₁₀mim BETI (H₂O < 1.79 mol % for C₆mim BMSI and 0.27 mol % for C₁₀mim BMSI³⁷) was measured for comparison (Table 2). No change in the orientation of the cation was measured, within the error of the experiment, suggesting that the amount of water in the sample has very little influence on the orientation of the imidazolium cation at the SiO₂ interface.

Interfacial Water Structure at the RTIL/SiO₂ Interface. The interfacial structure of water at the RTIL/SiO₂ interface was also investigated. The contribution due to water in the previous SFVS spectra of the RTILs was suppressed by performing the experiments on RTILs that were equilibrated with D₂O. The SFVS spectrum of bulk water at the water/SiO₂ interface is shown in Figure 8. In this spectrum, there are two broad peaks at 3200 and 3400 cm⁻¹ which have previously been assigned to the OH stretch of a highly coordinated “ice-like” water structure and a “liquid-like” bulk water structure, respectively.^{47,66} The imide-based RTILs contain a considerable amount of water, ranging between 9640 ppm (20.6 mol %) for C₆mim BMSI and 4820 ppm (14.0 mol %) for C₁₀mim BETI.³⁷ A representative SFVS spectrum of a water-equilibrated RTIL (C₁₀mim BETI) is also shown in Figure 8. This spectrum also shows the large broad bands at 3200 to 3400 cm⁻¹, similar to that seen at the water/SiO₂ interface.

Another important feature of the water-equilibrated RTIL SFVS spectrum is the observed interference of the C–H stretching modes within the water spectrum. From the spectrum in Figure 8, it is possible to determine the relative phase of the C–H stretching bands. The CH₂ ν_s, CH₃ ν_s, and HCCH ring stretches all appear as interferences (“dips”) within the bulk water spectrum, indicating that these vibrations are out of phase with the water background. The combination band centered at

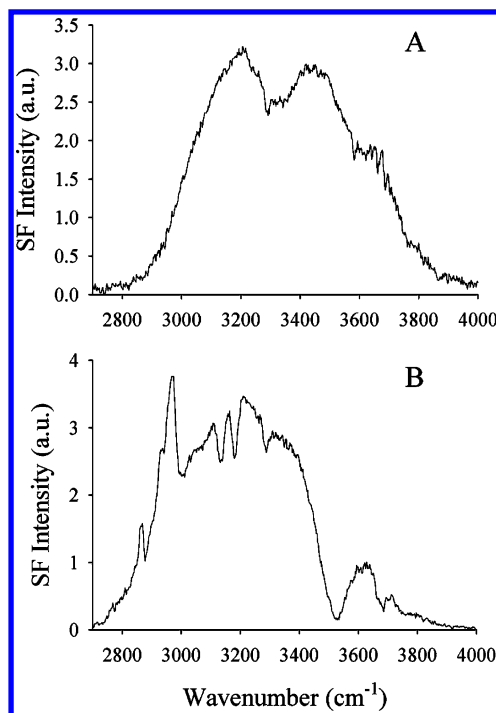


Figure 8. SFVS spectra (ssp) of the water/SiO₂ interface (A) and the water-equilibrated C₁₀mim BETI/SiO₂ interface (B).

~2975 cm⁻¹ appears as a peak on top of the bulk water spectrum, signifying that the vibrations in this band (Table 1) are in phase with the O–H stretches of water and out of phase with the other CH vibrations. These observations are consistent with the geometry of the imidazolium ring calculated above.

In addition to the water and C–H resonances observed, there are two additional interference peaks observed at ~3500 and ~3700 cm⁻¹. These interferences indicate that they are out of phase with the interfacial water background and are in phase with the other peaks in the CH stretching region. The peak at 3700 cm⁻¹ corresponds to the free OH.^{47,66} The peak at ~3500 cm⁻¹ is attributed to the O–H···N stretch of a water molecule hydrogen-bonded to the nitrogen of the anion. A similar frequency has been observed for FTIR studies of the BETI anion in polymer films of poly(propylene oxide).⁶⁷ Previous ATR-IR studies of imide-based RTILs have assigned similar peaks to hydrogen-bonded water molecules associated with the bis-(perfluoroalkylsulfonyl)imide anions in the RTIL.⁶⁸

Although SFVS spectra contain complex interference effects due to the physical nature of the nonlinear response, difference spectra can be used to retrieve information on relative spectral changes. The water-equilibrated RTIL spectra were subtracted from the spectrum of bulk water at the SiO₂ interface. Taking the difference spectra removes the contribution of the bulk water that has been adsorbed to the SiO₂ surface, which allows for a better understanding of the structure of the water molecules that are associated with the RTIL at the SiO₂ interface. A representative difference spectrum is shown in Figure 9 for C₁₀mim BETI. The O–H···N peak at 3500 cm⁻¹ and the free O–H peak at ~3700 cm⁻¹, which were destructively interfering with the H₂O background in Figure 8, now appear as positive resonances. The O–H···N peak has a shoulder at 3400 cm⁻¹, which was not clearly visible in the original spectrum. This shoulder arises from more liquid-like water in the water-equilibrated RTILs at the interface.

It has been suggested that the water, in similar imide-based RTILs, is predominantly hydrogen-bonded to the anions either as a single water molecule or in a dimeric complex with one

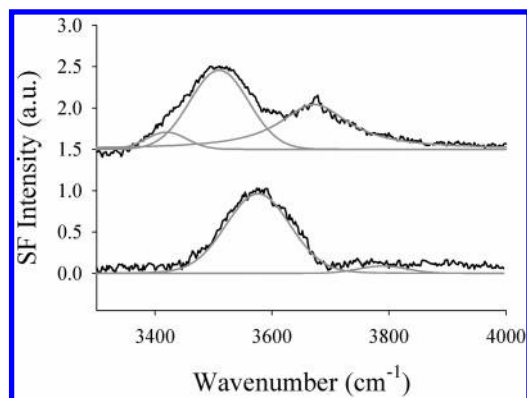


Figure 9. Difference spectra of water-equilibrated (top, offset by 1.5) and ambient (bottom) C₁₀mim BETI. Gray lines are fits to the spectra.

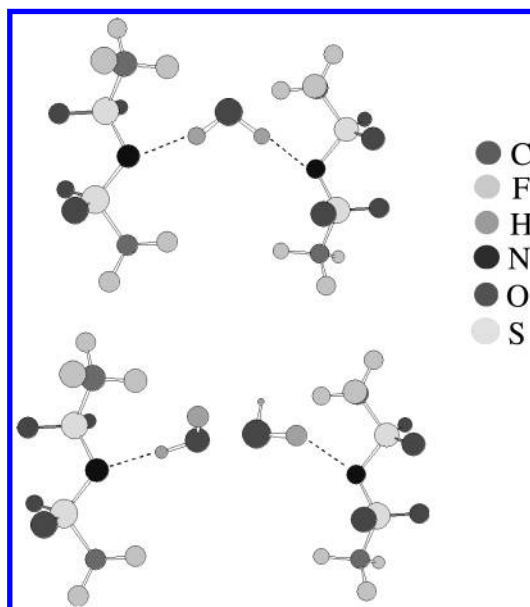


Figure 10. Structure of the bridging hydrogen-bonded water–anion complex (top) and the singly hydrogen-bonded water–anion complex (bottom) shown for the BMSI anion (see Figure 1).

water molecule bridging two anions (Figure 10).⁶⁸ The relative concentration of a singly versus doubly coordinated water molecule at the RTIL/SiO₂ interface can be obtained from the intensity of the free O–H resonance. A plot of the free O–H intensity, which has been normalized to the O–H···N stretch to account for experimental variations, versus the water content of the RTILs³⁷ is shown in Figure 11. The intensity of the free O–H increases as the water content of the RTILs increases. This result suggests that, at low concentrations of water in the RTIL, water associated with the anions at the interface is primarily bridging two anions. As the water concentration in the RTILs increases, there is an increase in the free O–H stretch, which suggests that more water molecules are hydrogen-bonded to a single anion.

The SFVS spectra of ambient RTILs also provide valuable information as to the nature of the water associated with the anions at the SiO₂ interface. The ambient water content of the imide-based RTILs is significantly less than the water-equilibrated RTILs. The water content of the ambient RTILs ranges from 79 ppm (0.0079% w/w, 0.27 mol %) for C₁₀-mimBETI to 732 ppm (0.073% w/w, 1.8 mol %) for C₆-mimBMSI. The SFVS difference spectrum of C₁₀mim BETI in contact with SiO₂ under ambient conditions is also shown in Figure 9. The spectrum is dominated by the O–H···N stretch

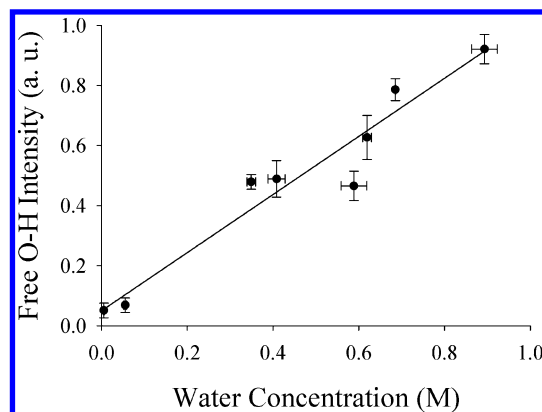


Figure 11. Free O–H intensity as a function of the bulk water content for the RTILs. The free O–H peak at 3700 cm⁻¹ has been normalized to the O–H···N peak at ~3500 cm⁻¹.

with very little free O–H. This fact supports the hypothesis that, at low water concentrations in the RTIL, H₂O is primarily hydrogen-bonded as a dimer (Figure 10). Comparing the water-equilibrated and ambient RTIL spectra in Figure 9, there is a shift in the peak frequencies of the O–H···N stretch of ~70 cm⁻¹. Similar frequency shifts have been observed previously and have been attributed to changes in the local environment of hydrogen-bonded water molecules.^{69–71}

Conclusions

SFVS was used to determine the orientation of the imidazolium cation at the RTIL/SiO₂ interface, as well as the structure of the interfacial water molecules. The measured tilt of the terminal alkyl –CH₃ group with respect to the surface normal was 25–42°. On the basis of an all-trans conformation of the alkyl chains, this orientation places the alkyl chain nearly parallel to the surface normal. The conformational order of the alkyl chains was also determined on the basis of the CH₂ ν_s/CH₃ ν_s ratio and was nearly identical for all the RTILs examined. The tilt of the imidazolium ring with respect to the surface normal was determined to be between 16 and 32° on the basis of the HCC dipole orientation. Surprisingly, the measured structure of the cation does not change significantly with either the composition of the RTIL or water content.

In addition to the interfacial structure of the cation, the organization of water at the surface was also determined. Nearly identical ice-like and “water-like” features were observed for both the water/SiO₂ surface and the RTIL/SiO₂ surface. Difference spectra revealed that the water molecules associated with the RTIL at the interface were hydrogen-bonded in either a monomer or a dimer configuration with the bis(perfluoroalkyl-sulfonyl)imide anions, consistent with previously IR studies of similar materials. A strong positive correlation between the free O–H intensity and the concentration of water in the bulk was observed, suggesting that the concentration of water in the bulk strongly influences the degree of hydration of the anions at the interface. These studies have allowed us to gain new insight into the structure of the imidazolium cation and water at the RTIL/SiO₂ interface and open the possibilities for the study of numerous other RTIL/solid and RTIL/liquid interfaces.

Acknowledgment. The authors thank the 3M Corporation for the generous donation of the LiBETI electrolyte. We would also like to thank Prof. Joel M. Harris and Dr. Rory H. “Ziggy” Uibel for assistance in performing the Raman studies of the RTILs. This work was supported by the Petroleum Research Fund (ACS PRF# 37628-G7).

References and Notes

- Quinn, B. M.; Ding, Z.; Moulton, R.; Bard, A. J. *Langmuir* **2002**, *18*, 1734–1742.
- Goldman, J. L.; McEwen, A. B. In *Proceedings of the Electrochemical Society*; Halpert, G., Gopikanth, M. L., Eds.; The Electrochemical Society: Pennington, NJ, 1999; Vol. 98-15, pp 507–519.
- Suarez, P. A. Z.; Consorti, C. S.; De Souza, R. F.; Dupont, J.; Goncalves, R. S. *J. Braz. Chem. Soc.* **2002**, *13*, 106–109.
- Schroder, U.; Wadhawan, J. D.; Compton, R. G.; Marken, F.; Suarez, P. A. Z.; Consorti, C. S.; de Souza, R. F.; Dupont, J. *New J. Chem.* **2000**, *24*, 1009–1015.
- Fuller, J.; Carlin, R. T.; Osteryoung, R. A. *J. Electrochem. Soc.* **1997**, *144*, 3881–3886.
- Fuller, J.; Carlin, R. T. In *Proceedings of the Electrochemical Society*; Trulove, P. C., Long, H. C. D., Stafford, G. R., Deki, S., Eds.; The Electrochemical Society: Pennington, NJ, 1998; Vol. 98-11, pp 227–230.
- McEwan, A. B.; Ngo, H. L.; LeCompte, K.; Goldman, J. L. *J. Electrochem. Soc.* **1999**, *146*, 1687–1695.
- Welton, T. *Chem. Rev.* **1999**, *99*, 2071–2083.
- Fischer, T.; Sethi, A.; Welton, T.; Woolf, J. *Tetrahedron Lett.* **1999**, *40*, 793–796.
- Okubo, K.; Shirai, M.; Yokoyama, C. *Tetrahedron Lett.* **2002**, *43*, 7115–7118.
- Earle, M. J.; McCormac, P. B.; Seddon, K. R. *Green Chem.* **1999**, *1*, 23–25.
- Carmichael, A. J.; Earle, M. J.; Holbrey, J. D.; McCormac, P. B.; Seddon, K. R. *Org. Lett.* **1999**, *1*, 997–1000.
- Sheldon, R. *Chem. Commun. (Cambridge)* **2001**, 2399–2407.
- Gordon, C. M. *Appl. Catal., A* **2001**, *222*, 101–117.
- Olivier, H. *J. Mol. Catal. A: Chem.* **1999**, *146*, 285–289.
- Seddon, K. R. *Kinet. Katal.* **1996**, *37*, 693–697.
- Dullius, J. E. L.; Suarez, P. A. Z.; Einloft, S.; de Souza, R. F.; Dupont, J.; Fischer, J.; De Cian, A. *Organometallics* **1998**, *17*, 815–819.
- Valkenberg, M. H.; deCastro, C.; Holderich, W. F. *Top. Catal.* **2001**, *14*, 139–144.
- Spear, S. K.; Visser, A. E.; Willauer, H. D.; Swatoski, R. P.; Griffin, S. T.; Huddleston, J. G.; Rogers, R. D. *ACS Symp. Ser.* **2001**, *766*, 206–221.
- Visser, A. E.; Swatoski, R. P.; Reichert, W. M.; Griffin, S. T.; Rogers, R. D. *Ind. Eng. Chem. Res.* **2000**, *39*, 3596–3604.
- Visser, A. E.; Holbrey, J. D.; Rogers, R. D. *Chem. Commun. (Cambridge)* **2001**, 2484–2485.
- Rogers, R. D.; Visser, A. E.; Swatoski, R. P.; Hartman, D. H. *Met. Technol. Beyond 2000: Proc. Symp.* **1999**, 139–147.
- Visser, A. E.; Reichert, W. M.; Swatoski, R. P.; Willauer, H. D.; Huddleston, J. G.; Rogers, R. D. *ACS Symp. Ser.* **2002**, *818*, 289–308.
- Huddleston, J. G.; Rogers, R. D. *Chem. Commun. (Cambridge)* **1998**, 1765–1766.
- Holbrey, J. D.; Visser, A. E.; Spear, S. K.; Reichert, W. M.; Swatoski, R. P.; Broker, G. A.; Rogers, R. D. *Green Chem.* **2003**, *5*, 129–135.
- Blancard, L. A.; Hancu, D.; Beckman, E. J.; Brennecke, J. F. *Nature (London)* **1999**, *399*, 28–29.
- Blanchard, L. A.; Brennecke, J. F. *Ind. Eng. Chem. Res.* **2001**, *40*, 287–292.
- Huddleston, J. G.; Visser, A. E.; Reichert, W. M.; Willauer, H. D.; Broker, G. A.; Rogers, R. D. *Green Chem.* **2001**, *3*, 156–164.
- Hagiwara, R.; Hirashige, T.; Tsuda, T.; Ito, Y. *J. Fluorine Chem.* **1999**, *99*, 1–3.
- Baker, S. N.; Baker, G. A.; Bright, F. V. *Green Chem.* **2002**, *4*, 165–169.
- Fletcher, K. A.; Storey, I. A.; Hendricks, A. E.; Pandey, S.; Pandey, S. *Green Chem.* **2001**, *3*, 210–215.
- Bonhote, P.; Dias, A.; Papageorgiou, N.; Kalyanasundaram, K.; Gratzel, M. *Inorg. Chem.* **1996**, *35*, 1168–1178.
- Visser, A. E.; Swatoski, R. P.; Rogers, R. D. *Green Chem.* **2000**, *2*, 1–4.
- Visser, A. E.; Swatoski, R. P.; Griffin, S. T.; Hartman, D. H.; Rogers, R. D. *Sep. Sci. Technol.* **2001**, *36*, 785–804.
- Hagiwara, R.; Ito, Y. *J. Fluorine Chem.* **2000**, *105*, 221–227.
- Ngo, H. L.; LeCompte, K.; Hargens, L.; McEwen, A. B. *Thermochem. Acta* **2000**, *357–358*, 97–102.
- Fitchett, B. D.; Knepp, T. N.; Conboy, J. C. *J. Electrochem. Soc.* **2004**, *151*, 219–225.
- Law, G.; Watson, P. R. *Chem. Phys. Lett.* **2001**, *345*, 1–4.
- Gannon, T. J.; Law, G.; Watson, P. R.; Carmichael, A. J.; Seddon, K. R. *Langmuir* **1999**, *15*, 8429–8434.
- Law, G.; Watson, P. R.; Carmichael, A. J.; Seddon, K. R. *Phys. Chem. Chem. Phys.* **2001**, *3*, 2879–2885.
- Neilson, G. W.; Adya, A. K.; Ansell, S. *Annu. Rep. Prog. Chem., Sect. C* **2002**, *98*, 273–322.
- Carmichael, A. J.; Hardacre, C.; Holbrey, J. D.; Nieuwenhuyzen, M.; Seddon, K. R. *Mol. Phys.* **2001**, *99*, 795–800.
- Abdul-Sada, A. a. K.; Greenway, A. M.; Hitchcock, P. B.; Mohammed, T. J.; Seddon, K. R.; Zora, J. A. *J. Chem. Soc., Chem. Commun.* **1986**, 1753–1754.
- Baldelli, S. *J. Phys. Chem. B* **2003**, *107*, 6148–6152; Rivera-Rubero, S.; Baldelli, S. *J. Phys. Chem. B* **2004**, *108*, 15133–15140.
- Abraham, M.; Abraham, M. C. *Electrochim. Acta* **2000**, *46*, 137–142.
- Tanaka, K.; Tamamushi, R. *J. Electroanal. Chem.* **1989**, *273*, 265–267.
- Miranda, P. B.; Shen, Y. R. *J. Phys. Chem. B* **1999**, *103*, 3292–3307.
- Wong, J. L.; Keck, J. H. *J. Org. Chem.* **1974**, *39*, 2398–2403.
- Dick, B.; Gierulski, A.; Marowsky, G.; Reider, G. A. *Appl. Phys. B* **1985**, *38*, 107–116.
- MacPhail, R. A.; Strauss, H. L.; Snyder, R. G.; Elliger, C. A. *J. Phys. Chem.* **1984**, *88*, 334–341.
- Snyder, R. G.; Strauss, H. L.; Elliger, C. A. *J. Phys. Chem.* **1982**, *86*, 5145–5150.
- O’Leary, T. J.; Levin, I. W. *J. Phys. Chem.* **1984**, *88*, 1790–1796.
- Bell, G. R.; Li, Z. X.; Bain, C. D.; Fischer, P.; Duffy, D. C. *J. Phys. Chem. B* **1998**, *102*, 9461–9472.
- Carter, D. A.; Pemberton, J. E. *J. Raman Spectrosc.* **1997**, *28*, 939–946.
- Perchard, C.; Novak, A. *Spectrochim. Acta, Part A* **1967**, *23*, 1953–1968.
- Frisch, M. J.; Trucks, G. W.; Schlegel, H. B.; Scuseria, G. E.; Robb, M. A.; Cheeseman, J. R.; Montgomery, J. A., Jr.; Vreven, T.; Kudin, K. N.; Burant, J. C.; Millam, J. M.; Iyengar, S. S.; Tomasi, J.; Barone, V.; Mennucci, B.; Cossi, M.; Scalmani, G.; Rega, N.; Petersson, G. A.; Nakatsuji, H.; Hada, M.; Ehara, M.; Toyota, K.; Fukuda, R.; Hasegawa, J.; Ishida, M.; Nakajima, T.; Honda, Y.; Kitao, O.; Nakai, H.; Klene, M.; Li, X.; Knox, J. E.; Hratchian, H. P.; Cross, J. B.; Adamo, C.; Jaramillo, J.; Gomperts, R.; Stratmann, R. E.; Yazyev, O.; Austin, A. J.; Cammi, R.; Pomelli, C.; Ochterski, J. W.; Ayala, P. Y.; Morokuma, K.; Voth, G. A.; Salvador, P.; Dannenberg, J. J.; Zakrzewski, V. G.; Dapprich, S.; Daniels, A. D.; Strain, M. C.; Farkas, O.; Malick, D. K.; Rabuck, A. D.; Raghavachari, K.; Foresman, J. B.; Ortiz, J. V.; Cui, Q.; Baboul, A. G.; Clifford, S.; Cioslowski, J.; Stefanov, B. B.; Liu, G.; Liashenko, A.; Piskorz, P.; Komaromi, I.; Martin, R. L.; Fox, D. J.; Keith, T.; Al-Laham, M. A.; Peng, C. Y.; Nanayakkara, A.; Challacombe, M.; Gill, P. M. W.; Johnson, B.; Chen, W.; Wong, M. W.; Gonzalez, C.; Pople, J. A. *Gaussian 03*, revision B.01; Gaussian, Inc.: Pittsburgh, PA, 2003.
- Zhang, D.; Gutow, J.; Eisenthal, K. B. *J. Phys. Chem.* **1994**, *98*, 13729–13734.
- Martin, J.; Montero, S. *J. Chem. Phys.* **1984**, *80*, 4610–4619.
- Ward, R. N.; Davies, P. B.; Bain, C. D. *J. Phys. Chem.* **1993**, *97*, 7141–7143.
- Duffy, D. C.; Davies, P. B.; Bain, C. D.; Ward, R. N.; Creeth, A. M. *Proc. SPIE-Int. Soc. Opt. Eng.* **1995**, *2547*, 342–351.
- Ward, R. N.; Duffy, D. C.; Davies, P. B.; Bain, C. D. *J. Phys. Chem.* **1994**, *98*, 8536–8542.
- Conboy, J. C.; Messmer, M. C.; Richmond, G. L. *J. Phys. Chem.* **1996**, *100*, 7617–7622.
- Miranda, P. B.; Pflumio, V.; Saijo, H.; Shen, Y. R. *J. Am. Chem. Soc.* **1998**, *120*, 12092–12099.
- Guyot-Sionnest, P.; Hunt, J. H.; Shen, Y. R. *Phys. Rev. Lett.* **1987**, *59*, 1597–1600.
- Hunt, J. H.; Guyot-Sionnest, P.; Shen, Y. R. *Chem. Phys. Lett.* **1987**, *133*, 189–192.
- Du, Q.; Freysz, E.; Shen, Y. R. *Phys. Rev. Lett.* **1994**, *72*, 238–241.
- Johansson, P.; Tegenfeldt, J.; Lindgren, J. *J. Phys. Chem. A* **2000**, *104*, 954–961.
- Miranda, P. B.; Kazarian, S. G.; Salter, P. A.; Welton, T. *Phys. Chem. Chem. Phys.* **2001**, *3*, 5192–5200.
- Richmond, G. L. *Chem. Rev.* **2002**, *102*, 2693–2724.
- DelBene, J. E.; Jordan, M. J. T. *Int. Rev. Phys. Chem.* **1999**, *18*, 119–162.
- Pimentel, G. C.; McClellan, A. L. *The Hydrogen Bond*; W. H. Freeman and Co.: San Francisco, CA, 1960.